JOURNAL OF MULTIFUNCTIONAL MATERIALS & PHOTOSCIENCE
12(2), December 2021, pp. 157-166

Cu^{2+} Adsorption of Magnetic Chitosan: Kinetic and Thermodynamic Studies

Xujie Peng[1], Liting Zhang[1*], Ruichang Cao[1], Meng Li[1], Xin Rong[1], Jianjun Li[1,2], Yin Liu[1,2]

[1]*Department of Materials Science and Engineering, Anhui University of Science and Technology, Huainan, China, 232001;*
[2]*Anhui International Joint Research Center for Nano Carbon-based Materials and Environmental Health, Huainan 232001, China*

Abstract: To improve the adsorption performance and solid-liquid separation of Cu^{2+} adsorbent, magnetic chitosan (MCS) adsorbent was fabricated via a chemical cross-linking method. The Cu^{2+} adsorption of MCS at 288, 298, and 308K was experimentally investigated and theoretically fitted by adsorption kinetic model, adsorption activation energy model, and adsorption isotherm model. The highest specific adsorption of the MCS for Cu^{2+} was tested as 38.7 mg/g. The kinetic model fitting result indicates that Cu^{2+} adsorption of MCS is more in consist with the pseudo-second-order kinetic model, suggesting that it is dominated by chemical adsorption. It is found that a two-step diffusion mechanism, the boundary layer diffusion followed by an intra-particle diffusion, may play an important role in Cu^{2+} adsorption. The adsorption activation energy is calculated as 10.05 kJ/mol, suggesting that physical adsorption has a significant effect on Cu^{2+} adsorption. From adsorption isotherm fitting the Cu^{2+} adsorption is found to belong to the Sips and Langmuir isothermal adsorption model. Based on all three fittings, it could be concluded that the Cu^{2+} adsorption of MCS is a composite adsorption process, which is dominated by chemical adsorption and supplemented by physical adsorption.

Keywords: *Magnetic chitosan; Cu^{2+} adsorption; Adsorption kinetics; Adsorption activation energy; Adsorption isotherm*

Introduction

With the rapid development of economic society and industrial production, the amount of industrial wastewater generated has increased significantly. As one of the main pollutants, industrial wastewater with heavy metal ions, including Cr^{6+}, Hg^{2+}, Cd^{3+}, Zn^{2+}, $Ni^{2+,}$ and Cu^{2+}, poses a high threat to the environment and human beings[1]. Because heavy metals cannot be excreted from the human body through physiological metabolism, the accumulation of heavy metals in the body will increase the risk of liver cancer and affect the human central nervous system[2]. To ensure human health and environmental safety, the heavy metal content in water must be strictly controlled below

* Corresponding author*: E-mail: ljj.hero@126.com*

the safe concentration threshold. Eg., the safety standard for Cu^{2+} is less than 0.5 mg/L. Most of the heavy metal wastewater is discharged from mineral production, electroplating, semiconductor manufacturing, and lead-acid battery industry. For example, the chemical mechanical polishing process in the semiconductor manufacturing industry produces heavy metal wastewater with a Cu^{2+} concentration over 100 mg/L[3]. After several treatment processes, the Cu^{2+} content was diluted, resulting in the production of a large amount of low concentration (tens of mg/L) Cu^{2+} wastewater[4; 5]. This concentration is still much higher than the allowable emission value. Therefore, the effective elimination of heavy metals from surface water and drinking water becomes an urgent task for humankind.

Many technologies, including coprecipitation, electrodialysis, membrane filtration, and ion exchange, have been explored to remove Cu^{2+} from water[3; 4; 6-8]. Some of these technologies are widely used in the wastewater treatment industry. Each method has specific water treatment ranges and advantages. However, they also have significant disadvantages, such as high cost, low efficiency, sludge handling problems, and possible secondary pollution. In addition, the removal efficiency for trace concentrations of Cu^{2+} is low. In contrast, adsorption is a more economical and feasible heavy metal removal technology, especially for low Cu^{2+} concentration wastewaters treatment. Furthermore, in this way, the adsorbed Cu^{2+} can be easily retrieved. The adsorption technique for Cu^{2+} removal has attracted significant interest. Various Cu^{2+} adsorbents were fabricated and studied, including activated carbon, lignin, silica composite, and zeolite[9-11]. Chitosan is a natural biopolymer, which has functional groups such as -OH and $-NH_2$ in the molecular. These groups have a chemical affinity for Cu^{2+} ions, thus can selectively adsorb Cu^{2+} from water[12; 13]. Furthermore, chitosan has the advantages of low cost, renewable, perfect hydrophilicity, biocompatibility, biodegradability, and non-toxicity[14; 15]. Therefore, chitosan is supposed as one of the best candidates for Cu^{2+} adsorbents. The other difficulty of adsorption technology is the low solid-liquid separation efficiency due to the tiny diameter of the adsorbents. To address this problem, the magnetic separation technique was introduced in[16]. Since most materials for adsorbents have no magnetic, a magnetic core is needed to make the adsorbent magnetic[16; 17]. Efficient solid-liquid separation could be achieved by using magnetic adsorbents.

In this study, magnetic chitosan (MCS) adsorbent was fabricated by using industrial waste coal-fly-ash magnetic spheres (MS) as magnetic core and chitosan as the coating. The structure and Cu^{2+} adsorption of MCS was investigated. The adsorption mechanism was carefully studied by three theoretical fitting models: adsorption kinetic model, adsorption activation energy model, and adsorption isotherm model.

1. Materials and methods

1.1 Materials

The coal-fly-ash used in this study was obtained from Luohe power plant in Huainan, China. Chitosan ($C_{56}H_{103}N_9O_{39}$, deacetylationÿ95%), Acetic Acid (CH_3COOH),

Glutaraldehyde ($C_5H_8O_2$), tween-80 ($C_{46}H_{52}N_5O_8P$), Copper(II) sulfate pentahydrate ($CuSO_4 \cdot 5H_2O$), DDTC ($C_5H_{10}NNaS_2$), ammonium hydroxide ($NH_3 \cdot H_2O$), concentrated hydrochloric acid (HCl, 32-38%), and sodium hydroxide (NaOH, 98%) were all purchased from Sinophenol Chemical Reagent Co., Ltd. (China). All the reagents were analytical reagent-grade.

The Cu-containing wastewater was prepared by dissolving $CuSO_4 \cdot 5H_2O$ in an appropriate amount of deionized water. The pH of the solution was adjusted by 0.1 M NaOH or HCl.

1.2 Equipments

CMS preparation equipment: Magnetic separation tube (GXG-08SD, Coal Research Institute, China), Planetary ball mill (XGB04, Nanjing Boyun Tong Co., Ltd.), Electronic balance (FA1004, Shanyu Hengping instrument). Cu^{2+} adsorption detection equipment: UV visible spectrophotometer (UV-5100, Shanghai Yuan analysis instrument Co., Ltd.), Constant temperature oscillator (ZQTY-70, Shanghai Zhichu Instrument Co., Ltd.). Structural characterization equipment: Scanning electron microscopy (SEM, ZEISS SUPRA 40, Germany), Fourier transform infrared (FT-IR) spectra in the range of 4000-400 cm^{-1} were recorded to determine the functional group of materials. Magnetic characterization equipment: HH-20 vibration sample magnetometer (VSM, Nanjing University Instrument Factory).

1.3 Preparation of MCS

The preparation of MS core includes multistage magnetic separation and ball milling. In short, MS were obtained from 100 mesh sieved coal fly ash by a magnetic separation under a 300 mT magnetic field. Then the MS was further separated under a low-intensity magnetic separation (100 mT), followed by a ball milling at 400 rpm for 10 h. The final MS particles were obtained by an additional low-intensity magnetic separation (100 mT).

The magnetic chitosan (MCS) was synthesized via a chemical cross-linking method. A certain amount of chitosan powder was dispersed in 80 mL 2% CH_3COOH solution and stirred for 10 min. Then tween-80 and a certain amount of CMS was added in proportion and stirred for 30 min. A certain amount of glutaraldehyde was added to the obtained gel and the solid content was separated by a permanent magnet, carefully washed with deionized water and ethanol. The product was dried at 60 ! in a vacuum drier for 12 h and sealed for later Cu^{2+} adsorption experiments.

1.4 Adsorption experiments

Cu^{2+} adsorption performance was investigated using homemade Cu-containing wastewater. 0.1 g MCS was added in iodide bottles containing 100 mL Cu^{2+} solution at concentrations in the range of 10-300 mg/L. The mixed solution oscillated in an oscillator under 288, 298, and 308 K, respectively, with a swing speed of 140 r/min. The

supernatant was extracted every 5 min for the following color reaction and a UV-Vis absorbance at 451 nm was measured. According to the standard adsorption curve of the Cu^{2+} solution, the Cu^{2+} concentration could be calculated from the absorbance value. Three parallel samples were taken for detection in each group of samples, and the average value was taken for analysis. The Cu^{2+} adsorption q was calculated according to formula (1).

$$q = \frac{(C_0 - C_e)v}{m} \quad (1)$$

where C_0 and C_e (mg/L) are the initial and final concentration of Cu^{2+}, respectively, v (L) is the volume of Cu^{2+} solution, and m (g) is the dosage of the adsorbent.

2. Results and discussion

2.1 Structural characterization and magnetic investigation

The structure of the MCS was characterized by SEM and FTIR. It is found the morphology of MCS changes a lot from that of CMS particles. As shown in Fig. 1(a) and (b), in the MCS sample, the CMS particles were fully covered by a certain substance. The FTIR investigation proves this substance is chitosan. As shown in Fig. 1(c), the absorption peaks at 1650 and 1080 cm^{-1} correspond to the C=O stretching vibration and the C-N axial bending vibration of amides in chitosan, indicating that chitosan has been coated on CMS. According to the VSM hysteresis loops, both CMS and MCS have a strong magnetism and small remanence and coercivity. The specific saturation magnetization of MCS is tested as 20.4 emu g^{-1}. Although the magnetism is low than CMS, it is also strong enough for effective magnetic separation.

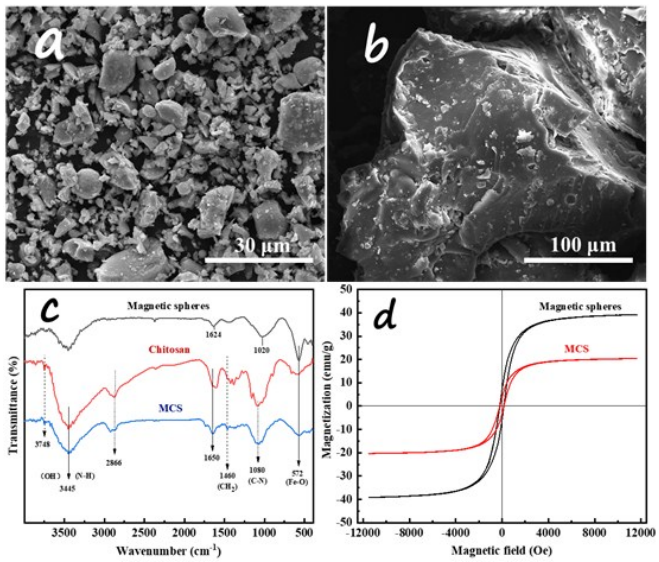

Figure.1 SEM of (a) CMS and (b) MCS, (c) FT-IR results of CMS, chitosan, and MCS, and (d) VSM hysteresis loop of CMS and MCS.

2.2 *Adsorption kinetics*

The Cu^{2+} adsorption performance of MCS was investigated by both experimental and theoretical fitting methods. Fig. 2 shows the Cu^{2+} adsorption performance and the kinetic fitting curve of the adsorption. The relevant fitting parameters are shown in Table. 1. The Cu^{2+} adsorption of MCS under 288, 298, and 308 K was tested as 13.3, 18.0, and 19.8 mg/g. It is found that the adsorption speed is first fast and then becomes slow gradually. In the first 5 minutes, more than 50% Cu^{2+} was removed from the solution. The Cu^{2+} adsorption capacity continued to increase slowly till saturating after 60 min around. The Cu^{2+} adsorption rate is closely related to the concentration of the surface chemical activity sites and the movement of Cu^{2+} ions. With the decrease of the reaction sites available for Cu^{2+} adsorption on the surface of the adsorbent, the adsorption reached equilibrium. The increase of adsorption with the rise of temperature may be due to the rise of the chemical activity sites and the increase of the collision chance between the adsorbents and the Cu^{2+} ions under higher temperatures.

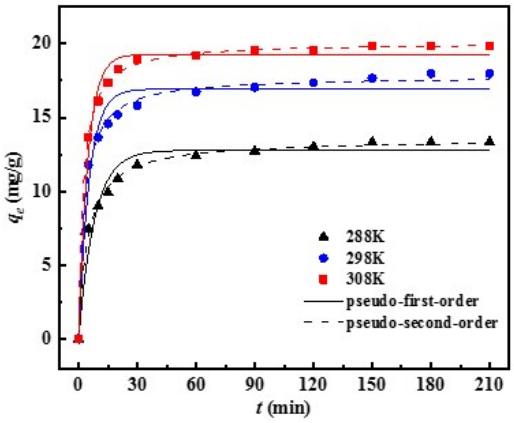

Figure. 2 Experimental Cu^{2+} adsorption performance and kinetic model fitting of CMS adsorbent.

The adsorption kinetics of Cu^{2+} on MCS was studied by using pseudo-first-order and pseudo-second-order kinetic models and intra-particle diffusion model. The pseudo-first-order and pseudo-second-order kinetic equations are respectively expressed as

$$q_t = q_e(1-e^{-k_1 t}) \tag{2}$$

$$q_t = \frac{k_2 q_e^2 t}{1+k_2 q_e t} \tag{3}$$

The initial adsorption rate v_0 (mg/g·min^{-1}) and half adsorption time $T_{1/2}$ (min) can be calculated using pseudo-second-order kinetic parameters. The relevant expressions are

$$v_0 = k_2 q_e^2 \tag{4}$$

$$t_{1/2} = \frac{1}{k_2 q_e} \tag{5}$$

The diffusion equation in the particle is shown in Equation (6):

$$q_t = k_{id} t^{1/2} + C_i \quad (6)$$

In equation (2)-(6), q_e and q_t (mg/g) are adsorption capacity at equilibrium concentration and predetermined time, k_1(min^{-1}), k_2 (g/mg·min^{-1}), and k_{id}(mg/g·min$^{1/2}$) are adsorption rate constants, and C_i is kinetic constant. As can be seen from Table. 1, the R^2 values of pseudo-second-order kinetics at 288, 298, and 308 K are 0.997, 0.995, and 0.999, respectively. Compared with those of pseudo-first-order kinetics, these values are closer to 1. It indicates that chemical adsorption plays a major role in adsorption, and physical adsorption also plays a certain role. With the increase of temperature, the initial adsorption rate (V_0) increased gradually (0.248, 0.343, and 0.567mg/g·min^{-1} for 288, 298, and 308 K, respectively), the semi-adsorption time ($T_{1/2}$) decreased significantly (11.62, 8.99, and 5.40min, respectively), and the equilibrium adsorption time shortened.

Table. 1 Kinetic parameters for adsorption of Cu^{2+} onto MCS composite.

T	$q_{e,exp}$	Pseudo-first-order			Pseudo-second-order				
		$q_{e,cal}$	k_1	R^2	$q_{e,cal}$	k_2	R^2	v_0	$t_{1/2}$
288	13.3	12.8	0.124	0.966	13.5	0.016	0.997	2.933	4.62
298	18.0	16.9	0.187	0.962	17.8	0.019	0.995	6.027	2.96
308	19.8	19.3	0.211	0.986	20.1	0.021	0.999	8.484	2.37

Fig. 3 is the three-segment line graph of q_t and $t_{1/2}$ for the intra-particle diffusion model. The adsorption process is divided into rapid surface adsorption, intra-particle diffusion, and the dynamic equilibrium of adsorption and desorption. Table. 2 shows that k_{1d}ÿk_{2d}ÿ k_{3d}, indicating that the diffusion rate of the boundary layer is greater than the diffusion rate within the particle and the equilibrium dynamic rate. Since the relationship between q_t and $t_{1/2}$ is nonlinear, and C_i is not zero, the Cu^{2+} adsorption could be controlled by a composite mechanism. Both boundary layer diffusion and intra-particle diffusion play an important role.

Table. 2 Intra-particle diffusion model parameters for adsorption of Cu^{2+} onto MCS composite.

T	$q_{e,exp}$	Intra-particle diffusion model								
		k_{1d}	C_1	R^2	K_{2d}	C_2	R^2	K_{3d}	C_3	R^2
288	13.3	2.94	0.201	0.984	1.13	5.64	0.979	0.149	11.3	0.913
298	18.0	4.49	0.395	0.974	0.756	11.7	0.979	0.199	15.2	0.980
308	19.8	5.29	0.415	0.979	0.929	13.9	0.934	0.094	18.6	0.882

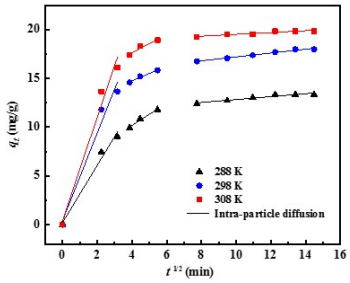

Figure. 3 Intra-particle diffusion model of MCS adsorption process.

2.3 Activation energy of adsorption

The adsorption activation energy (Ea) was obtained by using the fitted kinetic model rate constants and the Arrhenius formula (Eq. (7)).

$$ln\,(k) = ln\,(A) - \frac{E_a}{RT} \tag{7}$$

Where k is the adsorption rate constant, A is the pre-exponential influence factor, which is only related to the adsorption temperature. The rate constant used in this model is the rate constant k_2 of pseudo-second-order kinetics. Adsorption activation energy parameters are shown in Table.3.

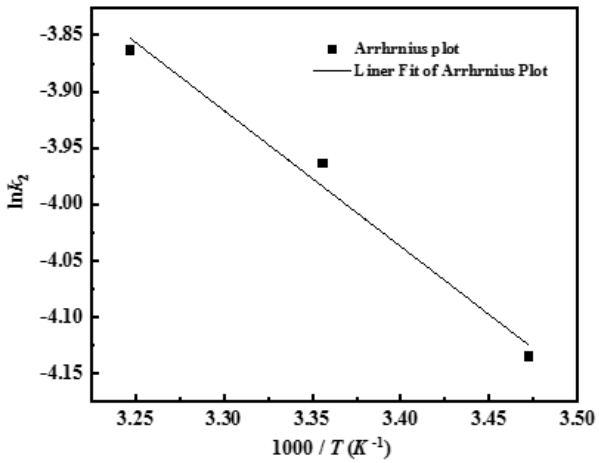

Figure. 4 Arrhenius equation fitting curve of MCS adsorption of Cu^{2+}.

As shown in Fig. 4, the activation energy of Cu^{2+} adsorption on MCS was 10.05 kJ/mol by calculating the slope of the fitting curve. The adsorption type can be judged by the strength of Ea: when 5<Ea<50 kJ/mol, it is a physical adsorption process; When 60<Ea<800 kJ/mol, it is a chemical adsorption process. Therefore, physical adsorption plays a major role in the Cu^{2+} adsorption of MCS.

Table. 3 Adsorption activation energy parameters of MCS adsorption of Cu^{2+}.

Arrhenius equation	R^2	Ea / (kJ mol^{-1})
$\ln(k_2) = -1209.187\frac{1}{T} + 0.073$	0.983	10.1

2.4 Adsorption isotherm model

Fig. 5 shows the effect of Cu^{2+} initial concentration on adsorption capacity at 288, 298, and 308K, respectively. When the initial concentration of Cu^{2+} is in the range of 10-300 mg/L, the adsorption capacity increases with the increase of the initial concentration of Cu^{2+}, and the higher the temperature, the greater the adsorption capacity. The maximum adsorption capacity was 38.7 mg/g.

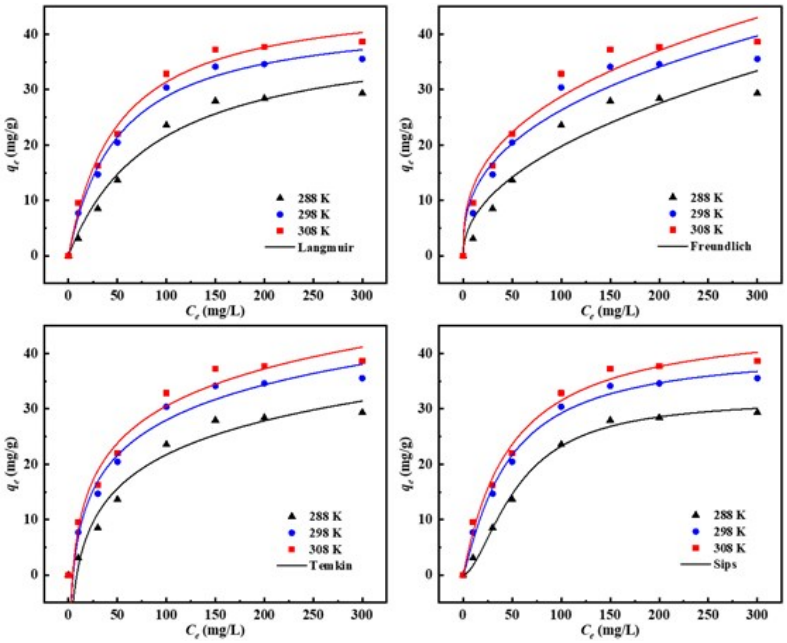

Figure. 5 Adsorption isotherms of Cu^{2+} on MCS at different temperatures.

Langmuir equation:

$$q_e = \frac{q_{max} k_L C_e}{1 + k_L C_e} \tag{8}$$

Freundlich equation:

$$q_e = k_F C_e^{1/n} \tag{9}$$

Temkin equation:

$$q_e = A \ln (k_T c_e) \tag{10}$$

Sips equation:

$$q_e = \frac{q_m k_s c_e^{\gamma}}{1 + k_s c_e^{\gamma}} \tag{11}$$

Where Ce (mg/L) is the concentration of Cu^{2+} in the solution at equilibrium, k_L (L/mg) is Langmuir adsorption coefficient, k_F (mg/g) and n are Freundlich adsorption isotherm constants, q_e and q_{max} (mg/g) represent the adsorption amount at equilibrium and the predicted maximum adsorption amount, respectively. The fitting curve of the adsorption model is shown in Fig. 5.

Table.4 Adsorption isotherm parameters of Cu^{2+} on MCS at different temperatures.

T	$q_{e,exp}$	Langmuir			Freundlich		
		q_m	k_L	R^2	k_F	1/n	R^2
288	29.4	40.8	0.0113	0.981	2.18	0.478	0.934
298	35.6	43.6	0.0194	0.991	4.68	0.375	0.952
308	38.7	47.0	0.0201	0.989	5.34	0.366	0.957
T	$q_{e,exp}$	Temkin			Sips			
		A	k_T	R^2	q_m	k_S	γ	R^2
288	29.4	8.82	0.118	0.972	31.9	1.21×10^{-3}	1.67	0.995
298	35.6	9.17	0.211	0.981	41.0	0.0124	1.15	0.992
308	38.7	9.69	0.234	0.979	46.3	0.0184	1.03	0.989

As shown in Table. 4, the validity of the isotherm model was tested according to the correlation coefficient (R^2). It can be seen that the adsorption process is in good agreement with Sips and Langmuir models, indicating that the adsorption process tends to be monomolecular adsorption and the surface of the adsorbent has a certain uniformity. Based on the experimental data and the fitting results of the three simulations, it can be concluded that the copper adsorption mechanism of MCS is dominated by monomolecular chemisorption, while physical adsorption also plays a key role.

3. Conclusion

In this work, MCS was fabricated via a chemical cross-linking method. The Cu^{2+} adsorption of the MCS composite was tested as 38.7 mg/g. Kinetics model, adsorption activation energy model, and isotherm model fittings were employed to study the mechanism of Cu^{2+} adsorption. Kinetic model fitting indicates that the Cu^{2+} adsorption of MCS is dominated by chemical adsorption. Diffusion simulation suggests that both the boundary layer diffusion and intra-particle diffusion have an important effect on Cu^{2+} adsorption. Adsorption isotherm fitting indicates that the Cu^{2+} adsorption of MCS could be a monomolecular force. While the Ea value obtained by adsorption activation energy fitting (10.1 kJ/mol) implies that physical adsorption plays an important role in Cu^{2+} adsorption. Combined with the results of the three fittings, it could be concluded that the adsorption process of Cu^{2+} by MCS is a combination of chemical adsorption and physical adsorption.

Acknowledgments

This work was financially supported by the Natural Science Foundation of Anhui Province, China (Grant No. 1908085ME127) and National Natural Science Foundation of China (Grant No. 51374015).

References

[1] Azimi A, Azari A, Rezakazemi M, et al. Removal of Heavy Metals from Industrial Wastewaters: A Review. ChemBioEng Reviews, 2017, 4(1): 37-59.

[2] Brewer G J. Copper toxicity in Alzheimer's disease: Cognitive loss from ingestion of inorganic copper. Journal of Trace Elements in Medicine and Biology, 2012, 26(2): 89-92.

[3] Lai C L, Lin S H. Electrocoagulation of chemical mechanical polishing (CMP) wastewater from semiconductor fabrication. Chemical Engineering Journal, 2003, 95(1): 205-211.

[4] Lai C L, Lin S H. Treatment of chemical mechanical polishing wastewater by electrocoagulation: system performances and sludge settling characteristics. Chemosphere, 2004, 54(3): 235-242.

[5] Hollingsworth J, Sierra-Alvarez R, Zhou M, et al. Anaerobic biodegradability and methanogenic toxicity of key constituents in copper chemical mechanical planarization effluents of the semiconductor industry. Chemosphere, 2005, 59(9): 1219-1228.

[6] Lin S H, Yang C R. Chemical and physical treatments of chemical mechanical polishing wastewater from semiconductor fabrication. Journal of Hazardous Materials, 2004, 108(1): 103-109.

[7] Zou S-W, How C-W, Chen J P. Photocatalytic Treatment of Wastewater Contaminated with Organic Waste and Copper Ions from the Semiconductor Industry. Industrial & Engineering Chemistry Research, 2007, 46(20): 6566-6571.

[8] Su Y-N, Lin W-S, Hou C-H, et al. Performance of integrated membrane filtration and electrodialysis processes for copper recovery from wafer polishing wastewater. Journal of Water Process Engineering, 2014, 4: 149-158.

[9] Razak M R, Yusof N A, Aris A Z, et al. Phosphoric acid modified kenaf fiber (K-PA) as green adsorbent for the removal of copper (II) ions towards industrial waste water effluents. Reactive and Functional Polymers, 2020, 147: 104466.

[10] Wang S, Wang K, Dai C, et al. Adsorption of Pb2+ on amino-functionalized core–shell magnetic mesoporous SBA-15 silica composite. Chemical Engineering Journal, 2015, 262: 897-903.

[11] Qin L, Feng L, Li C, et al. Amination/oxidization dual-modification of waste ginkgo shells as bio-adsorbents for copper ion removal. Journal of Cleaner Production, 2019, 228: 112-123.

[12] Anbinder P S, Macchi C, Amalvy J, et al. A study of the structural changes in a chitosan matrix produced by the adsorption of copper and chromium ions. Carbohydrate Polymers, 2019, 222: 114987.

[13] Li A, Lin R, Lin C, et al. An environment-friendly and multi-functional absorbent from chitosan for organic pollutants and heavy metal ion. Carbohydrate Polymers, 2016, 148: 272-280.

[14] Kandile N G, Mohamed H M, Mohamed M I. New heterocycle modified chitosan adsorbent for metal ions (II) removal from aqueous systems. International Journal of Biological Macromolecules, 2015, 72: 110-116.

[15] Gamal A, Ibrahim A G, Eliwa E M, et al. Synthesis and characterization of a novel benzothiazole functionalized chitosan and its use for effective adsorption of Cu(II). International Journal of Biological Macromolecules, 2021, 183: 1283-1292.

[16] Li J J, Dan H B, Xie W, et al. Synthesis and phosphorus adsorption of coal-fly-ash magnetic adsorbents. Chinese Journal of Inorganic Chemistry, 2018, 34(8): 1455-1462.

[17] Wu X F, Li J J, Zhu J B, et al. Advances in the resource utilization of fly ash magnetic micro-spheres. Materials Review, 2015, 29(23): 103-107.